Application of Neural Networks to Analyses of Nonlinearly Loaded Antenna Arrays Including Mutual Coupling Effects

Kun-Chou Lee, *Member, IEEE,* and Tsung-Nan Lin, *Senior Member, IEEE*

***Abstract*—In this paper, radial basis functions based neural networks (RBF-NN) are applied to the scattering of finite and infinite nonlinearly loaded antenna arrays including mutual coupling effects. The nodes in the input layer represent the parameters of antenna arrays or magnitudes of incident fields. There exist some nodes in the hidden layer for nonlinear mapping. The nodes in the output layer represent the magnitude of voltage at the input terminals of antennas at different harmonic frequencies. Numerical examples show that the scattering responses predicted by the trained RBF-NN models are very consistent with those calculated from the harmonic balance techniques. The trained RBF-NN models for the scattering of nonlinearly loaded antenna arrays are very efficient and the array mutual coupling effects are included.**

***Index Terms*—Loaded antenna, mutual coupling, neural networks (NN).**

I. Introduction

NONLINEAR lumped loads are often attached to the input terminals of antennas to yield the desired scattering characteristics. There have been many studies [1]–[9] for the analyses of a single nonlinearly loaded antenna element, including the time domain and the frequency domain methods. In [10]–[13], the analyses of a single nonlinearly loaded antenna are extended to the case of nonlinearly loaded antenna arrays. However, the treatments of nonlinearly loaded antenna arrays in [10]–[13] are time consuming due to the nonlinear characteristics of the lumped loads as well as the array mutual coupling effects. In practical applications, it is inefficient to directly apply the theoretical analyses of a single nonlinearly loaded antenna to the case of nonlinearly loaded antenna arrays. This motivates us to establish neural networks (NN) models for the scattering of nonlinearly loaded antenna arrays including mutual coupling effects. Although the training work of a neural network model is usually time consuming, it can be completed in advance.

Neural networks [14] have widespread applications in electromagnetics [15], [16]. According to [16], there are four main situations in which NN are good candidates for use in electromagnetics: 1) when the closed-form solution does not exist, and trial-and-error methods are the main approaches to tackling the problem at hand; 2) when an application requires real-time performance; 3) when faster convergence rates are required in the optimization of large systems; and 4) when enough measured data exist to train a neural network for prediction purpose, especially when no analytical tools exist. Obviously, the analysis of a nonlinearly loaded antenna array meets the above situations. However, there is still no research involving applications of NN in nonlinearly loaded antenna arrays. To our knowledge, this paper is the first study to apply NN to the scattering of nonlinearly loaded antenna arrays including mutual coupling effects.

In this paper, the radial basis functions based NN (RBF-NN) [14], [16] are applied to the scattering of finite and infinite nonlinearly loaded antenna arrays including mutual coupling effects. Currently, there is no closed-form solution for the scattering response of a nonlinearly loaded antenna array. Since NN are inherently nonlinear mapping models between input and output vectors, they can then be trained to predict the scattering responses of nonlinearly loaded antenna arrays. In our RBF-NN models, the nodes in the input layer represent the parameters of antenna arrays or magnitudes of incident fields. There exist some nodes in the hidden layer for nonlinear mapping. The nodes in the output layer represent the magnitude of voltage at the input terminals of antennas at different harmonic frequencies. Numerical examples show that the results predicted by the trained NN are in good agreement with those using the harmonic balance (HB) technique. Neural networks are very powerful. With the use of NN, the prediction for the scattering response of a nonlinearly loaded antenna array becomes very efficient and accurate, and the array mutual coupling effect is included.

In Section II, the HB analyses for nonlinearly loaded antenna arrays are investigated. In Section III, the RBF-NN models for nonlinearly loaded antenna arrays including mutual coupling effects are given. Numerical examples are shown in Section IV. Finally, the conclusion is given in Section V.

II. HB Techniques for Nonlinearly Loaded Antenna Arrays

The HB techniques for the analyses of a single nonlinearly loaded antenna have been investigated in [7], and are extended to the case of nonlinearly loaded antenna arrays in this section.

Consider an N-element nonlinearly loaded antenna array illuminated by a plane wave E_i, as shown in Fig. 1(a). Similar to

Manuscript received July 17, 2003; revised August 11, 2004. This work was supported by the National Science Council, Taiwan, R.O.C., under Grants NSC 93-2611-E-006-027 and NSC93-2213-E-002-057.

K.-C. Lee is with the Department of Systems and Naval Mechatronic Engineering, National Cheng-Kung University, Tainan 701, Taiwan, R.O.C. (e-mail: kclee@mail.ncku.edu.tw).

T.-N. Lin is with the Department of Electrical Engineering and the Graduate Institute of Communication Engineering, National Taiwan University, Taipei 106, Taiwan, R.O.C. (e-mail: tsungnan@cc.ee.ntu.edu.tw).

Digital Object Identifier 10.1109/TAP.2004.842695

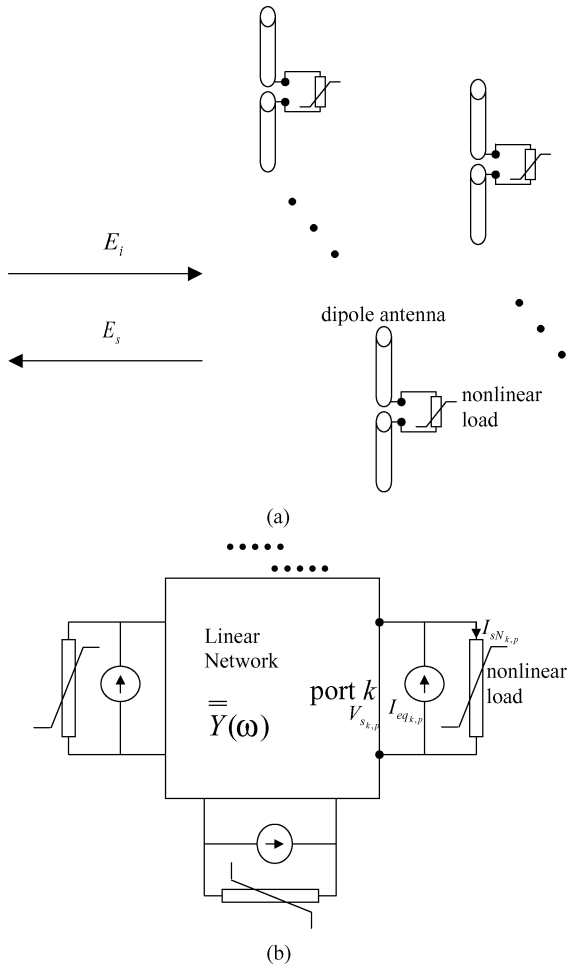

Fig. 1. (a) Schematic diagram of a finite nonlinearly loaded antenna array and (b) its equivalent microwave circuit.

the treatment in [10]–[13], the equivalent circuit of Fig. 1(a) can be expressed as an N-port network circuit, as shown in Fig. 1(b). In Fig. 1(b), see (1) shown at the bottom of the page, are voltages at the input terminals of the N antenna elements at different P harmonic frequencies, see (2) shown at the bottom of the page, are the short-circuit currents at antenna terminals due to the incident wave, see (3) shown at the bottom of the page, are the currents of the nonlinear load, and

$$\overline{\overline{Y}} = \begin{bmatrix} \overline{\overline{Y}}_{11} & \cdots & \overline{\overline{Y}}_{1N} \\ \vdots & \ddots & \vdots \\ \overline{\overline{Y}}_{N1} & \cdots & \overline{\overline{Y}}_{NN} \end{bmatrix} \tag{4}$$

is the matrix of antenna input admittances at different harmonic frequencies. The $\overline{\overline{Y}}_{ij}$ in (4) denotes the mutual admittances between the ith and the jth antenna elements at different harmonics. The circuit parameters of $\overline{\overline{Y}}$ and $\overline{I}_{\rm eq}$ in Fig. 1(b) can be obtained from the moment methods [17]. It should be noted that the mutual coupling effects of antenna arrays have been included in $\overline{\overline{Y}}$ [10]–[13].

The circuit equation is given as

$$\overline{\overline{Y}}\overline{V}_s - \overline{I}_{\rm eq} + \overline{\overline{D}} f(\overline{\overline{T}}\overline{V}_s) = \overline{0} \tag{5}$$

where the $f(\cdot)$ is the I-V characteristics of the nonlinear load. The $\overline{\overline{D}}$ and $\overline{\overline{T}}$ in (5) are the transformation matrix between time domain and frequency domain which are defined as

$$\begin{cases} \overline{v}_s(t) = \overline{\overline{T}}\overline{V}_s \\ \overline{I}_{sN} = \overline{\overline{D}}\overline{i}_{sN}(t) \end{cases}. \tag{6}$$

The HB technique [18] is then applied to find solution of $\overline{V}_s$ in (5). The resulting scattering responses can then be obtained from $\overline{V}_s$.

As a two-dimensional (2-D) infinite nonlinearly loaded antenna array illuminated by a plane wave E_i is considered, the analysis is similar to that given in [11]–[13]. The equivalent circuit and the analysis are just the same as the single element case except that the Green's function G_0 of a single antenna element is replaced by the 2-D infinite structure Green's function G_∞ in calculating the equivalent circuit parameters. The formulations of G_∞ are given in [11]–[13] in detail. Note that the array mutual coupling effects are included in G_∞.

In the above formulations, analyses of nonlinearly loaded antenna arrays are transformed into problems of microwave circuits that can be easily solved by the HB techniques and the array mutual coupling effects are included. In general, the

$$\overline{V}_s = [V_{s_{1,0}} \quad V_{s_{1,1}} \quad V_{s_{1,2}} \quad \cdots \quad V_{s_{1,2P-1}} \quad V_{s_{1,2P}} \quad ;\cdots\cdots\cdots; \quad V_{s_{N,0}} \quad V_{s_{N,1}} \quad V_{s_{N,2}} \quad \cdots \quad V_{s_{N,2P-1}} \quad V_{s_{N,2P}}]^T \tag{1}$$

$$\overline{I}_{\rm eq} = [0 \quad I_{{\rm eq}_{1,1}} \quad -I_{{\rm eq}_{1,2}} \quad \cdots \quad 0 \quad 0 \quad ;\cdots\cdots\cdots; \quad 0 \quad I_{{\rm eq}_{\rm N,1}} \quad -I_{{\rm eq}_{\rm N,2}} \quad \cdots \quad 0 \quad 0]^T \tag{2}$$

$$\overline{I}_{sN} = [I_{sN_{1,0}} \quad I_{sN_{1,1}} \quad I_{sN_{1,2}} \quad \cdots \quad I_{sN_{1,2P-1}} \quad I_{sN_{1,2P}} \quad ;\cdots\cdots\cdots; \quad I_{sN_{N,0}} \quad I_{sN_{N,1}} \quad I_{sN_{N,2}} \quad \cdots \quad I_{sN_{N,2P-1}} \quad I_{sN_{N,2P}}]^T \tag{3}$$

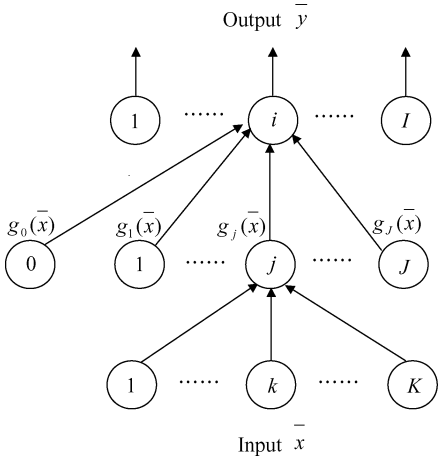

Fig. 2. Schematic diagram of a RBF-NN model.

numerical computations are complex since the parameters of the equivalent microwave circuit are obtained from moment methods. Due to the fast prediction characteristics of NN after they are trained in advance, the RBF-NN models are applied to this problem in the following section.

III. RBF-NN Models for Nonlinearly Loaded Antenna Arrays

In general, the HB technique is efficient for the analyses of simple microwave circuits. However, in practical applications, it is not efficient to directly apply the HB technique to the analyses of nonlinearly loaded antenna arrays due to the nonlinear characteristics of the lumped loads as well as the array mutual coupling effects. This motivates us to apply NN to the scattering of nonlinearly loaded antenna arrays including mutual coupling effects. Although the training work of a neural network model is usually time consuming, it can be completed in advance. The trained neural network models for the scattering of nonlinear loaded antenna arrays are very efficient and the array mutual coupling effects are included.

The models used in this study are the RBF-NN [14], [16]. As shown in Fig. 2, the output of the RBF-NN in the pth iteration loop can be expressed as

$$y_i(p) = w_{i0} + w_{i1}g_1(\overline{x}(p)) + w_{i2}g_2(\overline{x}(p)) + \cdots\cdots + w_{iJ}g_J(\overline{x}(p)) \quad (7)$$

for $i = 1, 2, \ldots\ldots, I$. The functions $g_j(\cdot)$, $j = 1, 2, \ldots\ldots, J$ in (7) represent the nonlinear transformations of input variables. In general, they are multivariate Gaussian functions defined as

$$g_j(\overline{x}) = \exp\left\{-\frac{1}{2}(\overline{x} - \overline{v}_j)^T \overline{\overline{\Sigma}}_j^{-1}(\overline{x} - \overline{v}_j)\right\} \quad (8)$$

where $\overline{v}_j$ is the mean vector and $\overline{\overline{\Sigma}}_j$ is the autocovariance matrix of the multivariate Gaussian function corresponding to hidden node j.

In this paper, the nodes in the input layer represent the parameters of antenna arrays or magnitudes of incident fields. There exist some nodes in the hidden layer for nonlinear mapping. The nodes in the output layer represent the magnitude of voltage at the input terminals of antennas at different harmonic frequencies. Initially, the RBF-NN model is trained by data sets obtained from the HB technique described in Section II. The learning strategy is given in detail in [14], [16]. After neural network models are trained, they can predict the scattering responses of nonlinearly loaded antenna arrays including mutual coupling effects.

IV. Numerical Examples

In this section, four numerical examples are given to verify the RBF-NN models described above. Without loss of generality, the dipole antennas are considered for simplicity since there is no limitation on the types of antennas. The incident wave has strength $E_i = 1.0$ V/m and propagates normally to the dipole antenna array. In all the four examples, the I-V characteristics of the lumped load at the input terminal of each dipole is described as

$$i = \frac{1}{75}v + 4v^3. \quad (9)$$

In the first example, a single element of nonlinearly loaded dipole antenna is considered. The dipole has a length-to-diameter ratio 74.2. The number of nodes in the input layer of the RBF-NN in Fig. 2 is set to be $K = 1$ which represents the ratio of dipole length to wavelength (L/λ). The number of nodes in the hidden layer of the RBF-NN in Fig. 2 is set to be $J = 6$ which is for the use of nonlinear mapping. The number of nodes in the output layer of the RBF-NN in Fig. 2 is set to be $I = 3$ which represents the magnitude of voltage at the antenna input terminal at harmonic frequencies ω, 2ω, and 3ω, where ω is the angular frequency of the incident wave. In the learning phase, 101 training data sets calculated from the HB technique, as described in Section II, are used to train the RBF-NN model. The ratios of L/λ for the training data sets are randomly selected in the interval of [0.3, 1.3]. After the RBF-NN is trained, it can predict the magnitude of voltage at the antenna input terminal at harmonic frequencies ω, 2ω, and 3ω, for different values of L/λ. In the predicting phase, there are also another 101 prediction points (different from the training points) with the ratios of L/λ uniformly distributed in the interval of [0.3, 1.3]. Fig. 3 shows the magnitude of voltage at the input terminal of a single nonlinearly loaded antenna for different dipole lengths at harmonic frequencies ω, 2ω, and 3ω predicted by the neural network model. For comparison, the results calculated from the HB techniques are also given in Fig. 3. It shows that they are in good agreement. In addition, as we convert the antenna terminal voltages in Fig. 3 into RCS (radar cross section), the results are found to be consistent with those given in [13] (genetic algorithm based analyses).

In the second example of finite antenna array, a two-element parallel nonlinearly loaded dipoles array is considered. Each element is the same as that given in the first example. The dipole length is chosen as 0.467 λ. Due to the symmetry of the two array elements, the induced voltage and the current distribution of each dipole are the same. The neural network model

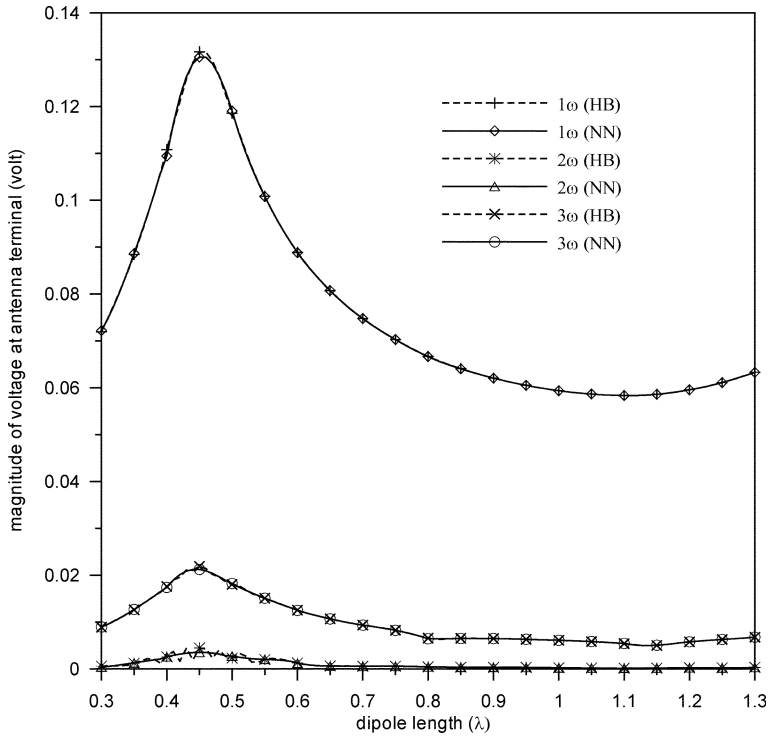

Fig. 3. Magnitude of voltage at the input terminal of a single nonlinearly loaded antenna for different dipole length at different harmonic frequencies of 1ω, 2ω, and 3ω. (NN models; HB techniques).

is then the same as that given in the first example except that the input node represents the spacing of array elements. The RBF-NN is trained by 101 data sets calculated from the harmonic balance technique, as described in Section II. The element spacing of these training data sets is randomly selected in the interval of $[0.3\lambda, 1.3\lambda]$. After the neural network model is trained, it can predict the scattering responses for different values of array element spacing. In the predicting phase, there are also 101 prediction points (different from the training points) with the element spacing uniformly distributed in the interval of $[0.3\lambda, 1.3\lambda]$. Fig. 4 shows the magnitude of voltage at the input terminal of each dipole antenna for different array element spacing at harmonic frequencies ω, 2ω, and 3ω predicted by the neural network model. For comparison, the results calculated from the harmonic balance techniques are also given in Fig. 4. It shows that they are in good agreement. These results are also consistent with those given in [13] which exploits the genetic algorithm to compute the same problem with element spacing of 0.75 λ.

In the third example of infinite antenna array, a 2-D rectangular infinite array structure lying in the x-y plane is considered. Each antenna element is the same as that given in the second example. As described in [11]–[13], the induced voltage and the current distribution of each dipole in an infinite array structure are the same. For simplicity, the array element spacing in the $\hat{x}$-direction and in the $\hat{y}$-direction are assumed to be equal. Therefore, the neural network model is the same as that given in the second example. The RBF-NN is trained by 101 data sets calculated from harmonic balance techniques of a single nonlinearly loaded antenna element by using the infinite periodic structure Green's function, in which Poisson sum technique is applied and the mutual coupling effects are included in the resulting Green's function, as those given in [11]–[13]. The generation of the training data sets and the prediction points is similar to that given in the previous examples. Fig. 5 shows the magnitude of voltage at the input terminal of each dipole antenna for different array element spacing at harmonic frequencies ω, 2ω, and 3ω predicted by the neural network model. For comparison, the results calculated from the harmonic balance techniques together with the infinite periodic structure Green's functions are also given in Fig. 5. It shows that they are in good agreement. These results are also consistent with those given in [13] which exploits the genetic algorithm to compute the same problem with element spacing of 0.75 λ.

It is very well known that nonlinear problems are very sensitive to the signal level. As different magnitudes of incident fields in the first example (a single element of nonlinearly loaded dipole antenna) are considered, an additional node in the input layer is required to account for field magnitudes. In the learning phase, $101 \times 91 = 9191$ training data sets, i.e., 101 sets of L/λ randomly selected in the interval of [0.3, 1.3] and 91 sets of E_i randomly selected in the interval of [0.1, 1.0], calculated from the harmonic balance techniques are used to train the RBF-NN model. In the predicting phase, there are also $101 \times 91 = 9191$ prediction points (different from the training points) with uniformly distributed dipole lengths and uniformly distributed incident field strengths. Fig. 6 shows the magnitude of voltage at the input terminal of a single nonlinearly loaded antenna for different dipole lengths and different magnitudes of incident fields at the fundamental frequency using NN models and the harmonic balance techniques. It shows that they are in good agreement.

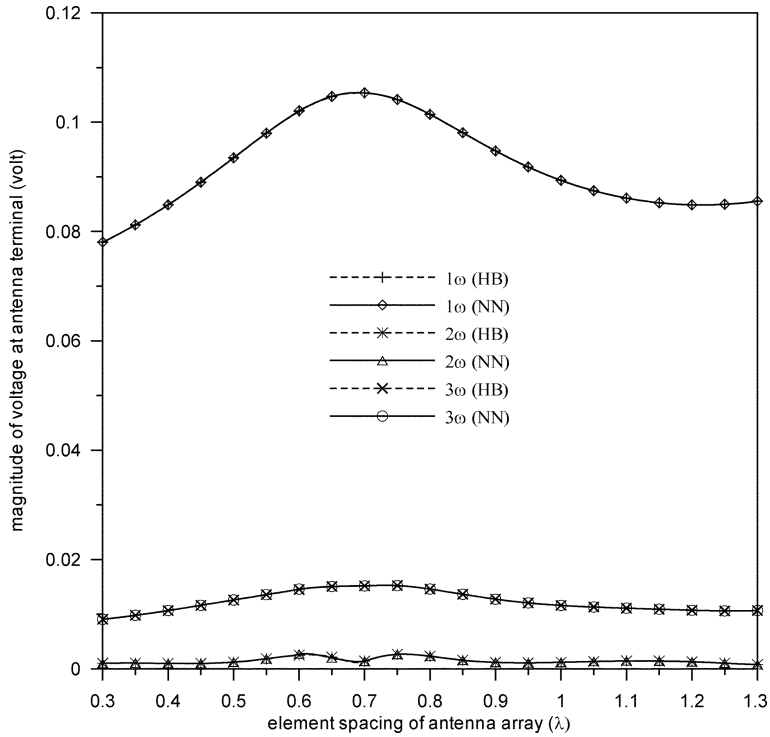

Fig. 4. Magnitude of voltage at each input terminal of a nonlinearly loaded antenna array with two parallel dipoles for different array element spacing at different harmonic frequencies of 1ω, 2ω, and 3ω. (NN models; HB techniques).

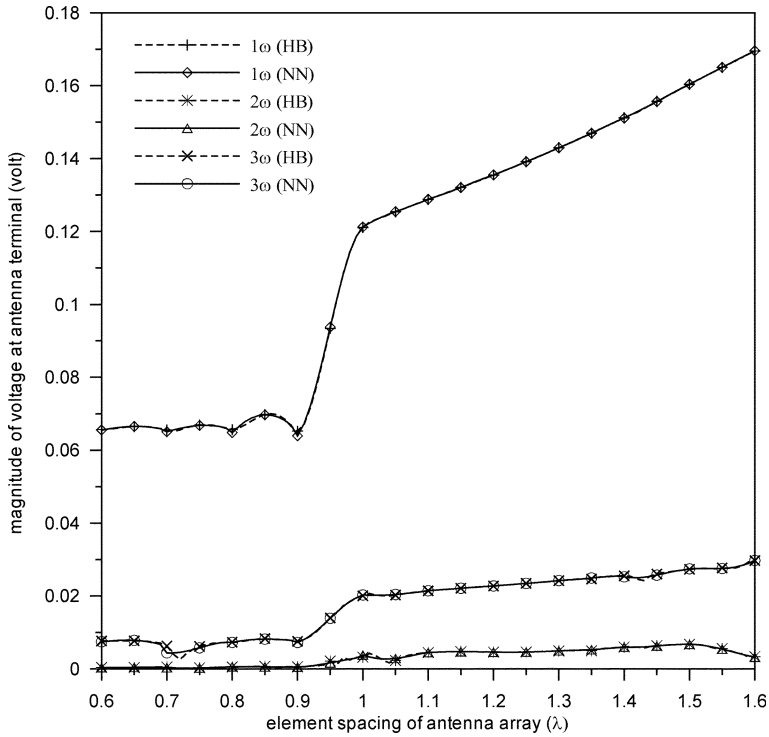

Fig. 5. Magnitude of voltage at each input terminal of a nonlinearly loaded antenna array with a 2-D rectangular infinite array structure lying in the x-y plane for different array element spacing at different harmonic frequencies of 1ω, 2ω, and 3ω. (NN models; HB techniques).

The above numerical computations in this study are performed using a PC with Intel Pentium 2 GHz CPU. The time required to producing a training data set using the formulations of Section II is about 1.5 s. It should be noted that these training data sets can also be obtained from measurement in practical engineering applications. In dealing with the RBF-NN, the learning rate is set to be 0.1 and the maximum learning loops are set to be 40 000. All the input and output variables are normalized into values in the range of [0.0 , 1.0] during the neural computing. The time required to train the neural network is

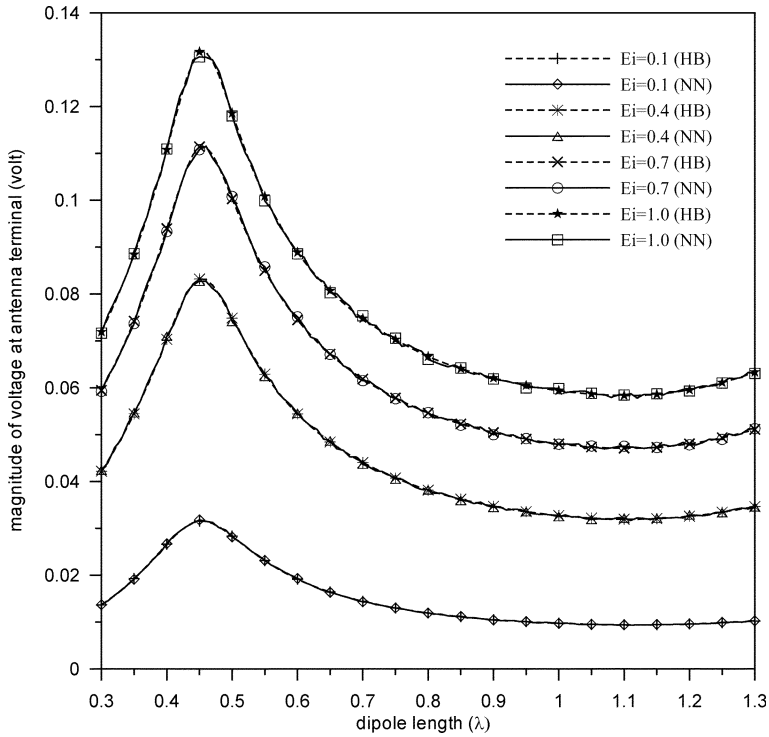

Fig. 6. Magnitude of voltage at the input terminal of a single nonlinearly loaded antenna for different dipole lengths ($L/\lambda = 0.3$ to 1.3) and different magnitudes of incident fields ($E_i = 0.1$ to 1.0 V/m) at the fundamental harmonic frequency. (NN models; HB techniques).

about 20 s for the first, the second and the third examples, and is about 34 min for the fourth example. Although the training time increases with the size of NN, it can be completed in advance. In fact, the main advantage of using NN in electromagnetics is the rapidity in the prediction phase. It is almost real-time in the prediction phase of NN. In addition, the prediction error for every numerical example given above is within 1% which is accurate from the engineering point of view.

The nonlinear phenomena of scattering responses are shown in Figs. 3–5. As described in [13], due to the linear term of $f(\cdot)$ in (9), the voltage component at fundamental frequency ω is much greater than those of the higher order mixing frequencies. In addition, the voltage component at mixing frequency 3ω is slightly greater than that at mixing frequencies 2ω. This is due to the effect of the cubic term of $f(\cdot)$ in (9). It should be noted that there exist no limitation on the I-V characteristics for nonlinear lumped loads of each antenna element. In this study, the nonlinear characteristics for each lumped load is assumed to have the form as (9) which is the same as that used in [13] so that the results of [13] can be used for comparison.

In order to show the performance of the RBF-NN models in this study, different neural network architectures trained by various learning algorithms are compared in this section. For simplicity, the first numerical example described above is considered. Fig. 7 shows the average prediction errors of prediction data sets at different harmonic frequencies by using RBF-NN, and multilayered perceptron neural network (MLP-NN) architectures trained by the Levenberg–Marquardt method, the resilient back-propagation method, and the gradient descent method. It should be noted that the prediction error in Fig. 7 is defined as the absolute value of the difference between the predicted output and the desired output. All the MLP-NN architectures are with the same size, learning rate, and maximum training loops as those given for the RBF-NN model described above. From Fig. 7, it shows that the results predicted by RBF-NN are with smaller average errors than

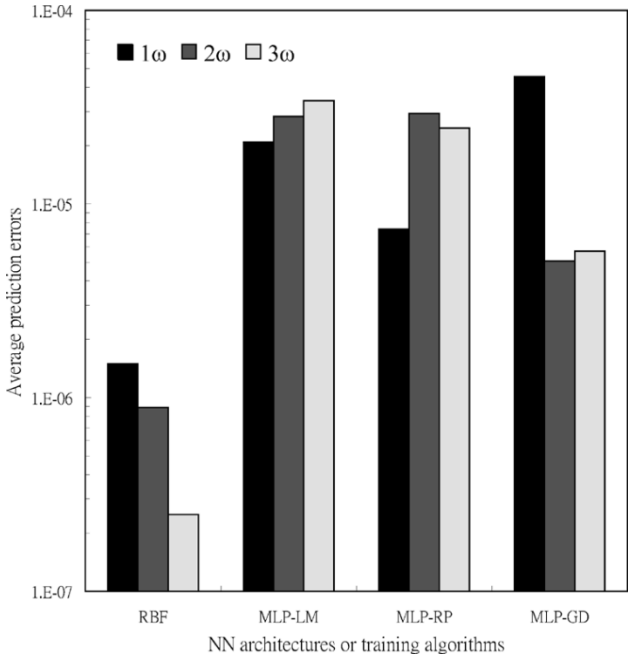

Fig. 7. Average prediction errors of prediction data sets at different harmonic frequencies by using RBF-NN (denoted as "RBF"), and MLP-NN architectures trained by the Levenberg–Marquardt method (denoted as "MLP-LM"), the resilient back-propagation method (denoted as "MLP-RP"), and the gradient descent method (denoted as "MLP-GD").

other neural network models. This convinces us that the use of RBF-NN architecture is suitable in problems of nonlinearly loaded antennas.

V. Conclusion

In this paper, the RBF-NN models are applied to predict the scattering responses of finite and infinite nonlinearly loaded antenna arrays at different harmonic frequencies. Since the RBF-NN model is inherently one type of the general regression [19], it can predict new results nonlinearly from some training data sets. With the use of NN, the complex numerical computation for the analysis of a nonlinearly loaded antenna array can be replaced by a very simple algebraic operation as the NN are well trained. Numerical examples show that the results predicted by the RBF-NN models are consistent with those calculated from the harmonic balance techniques in [7] and genetic algorithms based analyses in [13]. Although the training work of a RBF-NN model is usually time consuming, it can be completed in advance. The trained RBF-NN models for predicting the scattering responses of nonlinearly loaded antenna arrays including mutual coupling effects are very efficient and thus useful in the applications of antenna design, remote sensing, and wireless communication.

Acknowledgment

The authors would like to express their sincere gratitude to Prof. T.-H. Chu, Department of Electrical Engineering, National Taiwan University, Taipei, Taiwan, R.O.C., and Prof. C.-C. Huang, Department of Electrical Engineering, Yuan-Ze University, Taoyuan, Taiwan, R.O.C., for their helpful discussions.

References

[1] H. K. Schuman, "Time-domain scattering from a nonlinearly loaded wire," *IEEE Trans. Antennas Propag.*, vol. AP-22, no. 4, pp. 611–613, Jul. 1974.

[2] J. J. Nahas, "Modeling and computer simulation of a microwave-to-dc energy conversion element," *IEEE Trans. Microwave Theory Tech.*, vol. MTT-23, no. 12, pp. 1030–1035, Dec. 1975.

[3] T. K. Sarkar and D. D. Weiner, "Scattering analysis of nonlinearly laded antennas," *IEEE Trans. Antennas Propag.*, vol. AP-24, no. 2, pp. 125–131, Mar. 1976.

[4] T. K. Liu and F. M. Tesche, "Analysis of antennas and scatterers with nonlinear loads," *IEEE Trans. Antennas Propag.*, vol. AP-24, no. 2, pp. 131–139, Mar. 1976.

[5] J. A. Landt, "Network loading of thin-wire antennas and scatterers in the time domain," *Radio Sci.*, vol. 16, pp. 1241–1247, Nov. 1981.

[6] J. A. Landt, E. K. Miller, and F. J. Deadrick, "Time domain modeling of nonlinear loads," *IEEE Trans. Antennas Propag.*, vol. AP-28, no. 1, pp. 121–126, Jan. 1983.

[7] C. C. Huang and T. H. Chu, "Analysis of wire scatterers with nonlinear or time-harmonic loads in the frequency domain," *IEEE Trans. Antennas Propag.*, vol. 41, no. 1, pp. 25–30, Jan. 1993.

[8] R. Luebbers, J. Beggs, and K. Chamberlin, "Finite difference time-domain calculation of transients in antennas with nonlinear loads," *IEEE Trans. Antennas Propagat.*, vol. 41, pp. 566–573, May 1993.

[9] J. A. Porti and J. A. Morente, "A numerical analysis of wire antennas loaded with varistor-composite materials," *IEEE Trans. Electromagn. Compat.*, vol. 36, no. 1, pp. 23–31, Feb. 1994.

[10] K. C. Lee, "An efficient algorithm for the steady-state analysis of a nonlinearly loaded antenna array," *J.Electromagn. Waves Applicat.*, vol. 14, pp. 1373–1382, 2000.

[11] ——, "Analysis of large nonlinearly loaded antenna arrays under multitones excitation," *Microw. Opt. Technol. Lett.*, pp. 319–323, Jun. 2000.

[12] ——, "Two efficient algorithms for the analyses of a nonlinearly loaded antenna and antenna array in the frequency domain," *IEEE Trans. Electromagn. Compat.*, vol. 45, no. 4, pp. 339–346, Nov. 2000.

[13] ——, "Genetic algorithms based analyses of nonlinearly loaded antenna arrays including mutual coupling effects," *IEEE Trans. Antennas Propag.*, vol. 51, no. 4, pp. 776–781, Apr. 2003.

[14] S. Haykin, *Neural Networks—Comprehensive Foundation*. Englewood Cliffs, NJ: Prentice-Hall, 1999.

[15] Q. J. Zhang and K. C. Gupta, *Neural Networks for RF and Microwave Design*. Boston, MA: Artech House, 2000.

[16] C. Christodoulous and M. Georgiopoulos, *Applications of Neural Networks in Electromagnetics*. Boston, MA: Artech House, 2001.

[17] R. F. Harrington, *Field Computation by Moment Methods* New York, Macmillan, 1968.

[18] S. A. Mass, *Nonlinear Microwave Circuits*. Dedham, MA: Artech House, 1988, ch. 3.

[19] D. F. Specht, "A general regression neural network," *IEEE Trans. Neural Netw.*, vol. 2, pp. 568–576, Aug. 1996.

Kun-Chou Lee (M'00) was born in Chia-yi, Taiwan, R.O.C., in 1966. He received the B.S., M.S., and Ph.D. degrees, all in electrical engineering, from National Taiwan University, Taipei, Taiwan, R.O.C., in 1989, 1991, 1995, respectively.

From 1995 to 1997, he was in the Taiwan army. From 1997 to 2003, he was with the faculty of the Wu-Feng Institute of Technology, Shu-Te University, Taiwan, R.O.C., and National Kaohsiung University of Applied Sciences, Taiwan, R.O.C. Since 2004, he has been with the faculty of the Department of Systems and Naval Mechatronic Engineering, National Cheng-Kung University, Tainan, Taiwan, R.O.C., where he is now an Associate Professor. His research interests include microwave imaging, antennas, microwave circuits, and application of wireless technologies in land, oceanic, and underwater environments.

Tsung-Nan Lin (SM'03) received the B.S. degree in electrical engineering from National Taiwan University, Taipei, Taiwan, R.O.C. in 1989, and the M.A. and Ph.D. degrees in electrical engineering from Princeton University, Princeton, NJ, in 1993 and 1996, respectively.

He was a Teaching Assistant with the Department of Electrical Engineering, Princeton University, from 1991 to 1992. From 1992 to 1996, he was a Research Assistant with NEC Research Institute. He has been with EPSON R&D Incorporated and EMC. Since February 2002, he has been with the Department of Electrical Engineering and the Graduate Institute of Communication Engineering, National Taiwan University.

Dr. Lin is a Member of Phi Tau Phi scholastic honor society.